2D Materials

RECEIVED
29 September 2016

REVISED
4 December 2016

ACCEPTED FOR PUBLICATION
13 December 2016

PUBLISHED
25 January 2017

PAPER

Effective elastic properties of two dimensional multiplanar hexagonal nanostructures

T Mukhopadhyay[1,3], A Mahata[2], S Adhikari[1] and M Asle Zaeem[2]

[1] College of Engineering, Swansea University, Swansea, UK
[2] Department of Materials Science and Engineering, Missouri University of Science and Technology, Rolla, MO, USA
[3] Author to whom any correspondence should be addressed.

E-mail: 800712@swansea.ac.uk (T Mukhopadhyay), akm6w3@mst.edu (A Mahata), S.Adhikari@swansea.ac.uk (S Adhikari) and zaeem@mst.edu (M Asle Zaeem)

Keywords: hexagonal nano-structures, graphene, hBN, stanene, MoS_2, analytical closed-form formulae, effective elastic modulus

Abstract

A generalized analytical approach is presented to derive closed-form formulae for the elastic moduli of hexagonal multiplanar nano-structures. Hexagonal nano-structural forms are common for various materials. Four different classes of materials (single layer) from a structural point of view are proposed to demonstrate the validity and prospective application of the developed formulae. For example, graphene, an allotrope of carbon, consists of only carbon atoms to form a honeycomb like hexagonal lattice in a single plane, while hexagonal boron nitride (hBN) consists of boron and nitrogen atoms to form the hexagonal lattice in a single plane. Unlike graphene and hBN, there are plenty of other materials with hexagonal nano-structures that have the atoms placed in multiple planes such as stanene (consists of only Sn atoms) and molybdenum disulfide (consists of two different atoms: Mo and S). The physics based high-fidelity analytical model developed in this article are capable of obtaining the elastic properties in a computationally efficient manner for wide range of such materials with hexagonal nano-structures that are broadly classified in four classes from structural viewpoint. Results are provided for materials belonging to all the four classes, wherein a good agreement between the elastic moduli obtained using the proposed formulae and available scientific literature is observed.

1. Introduction

The fascinating properties of graphene has initiated an enormous interest among the scientific community for exploration of prospective alternative two-dimensional materials that could possess exciting electronic, optical, thermal, chemical and mechanical characteristics [1–3]. The intense research in quasi-two-dimensional materials started with feasible isolation of the single layer carbon atoms [4]. Over the last decade the interest in this quasi-two-dimensional family of materials has expanded from hexagonal boron nitride (hBN), BCN, graphene oxides to Chalcogenides like MoS_2, $MoSe_2$ and other two dimensional materials like stanene, silicene, sermanene, phosphorene, borophene etc [5, 6]. It is however necessary to study these materials at nano-scale as most of the fascinating characteristics are in atomic scale and single layer forms [7]. Among different such materials, as discussed above, hexagonal nano-structure is a very prominent structural form [2]. The common practises to investigate these materials are first principle studies/ *ab initio* [8–10], molecular dynamics [11] and molecular mechanics [12], which can reproduce the results of experimental analysis with an expense of economically expensive and time consuming supercomputing facilities. Analytical models leading to closed form formulae are presented by many researchers for materials having hexagonal nano-structures such as graphene [13, 14] and hBN [15]. An informative study is recently reported considering analytical mechanical characterization of different such hexagonal monoplanar structural forms [16]. This approach of mechanical property characterization is computationally very efficient, yet accurate. However, the analytical models for hexagonal nano-structures developed so far are limited to monoplanar structural forms, where all the atoms stay in a single plane. Most of the quasi-two-dimensional materials, as discussed above, posses a structural form where the atoms are found to be placed in multiple planes as shown in figure 1. From the figure it is quite evident that even though the nano-structure has a hexagonal top view, two different atoms (indicated by two different colors) are placed in different planes (three planes can be

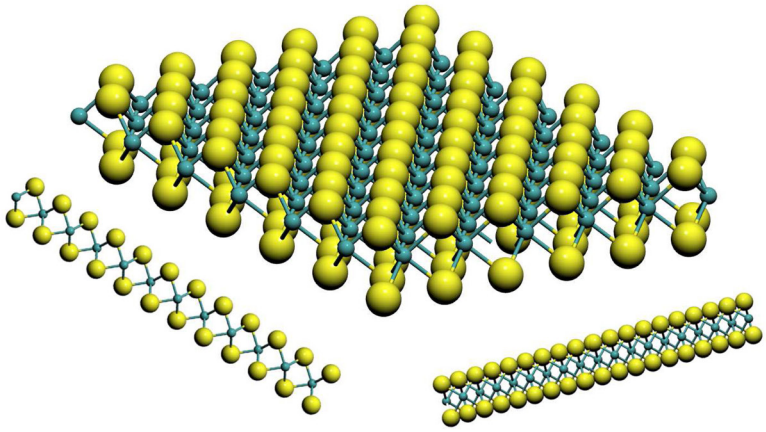

(a)

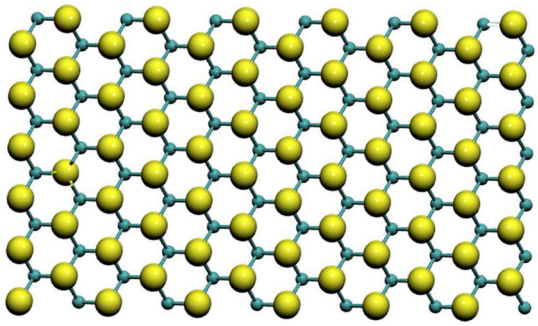

(b)

Figure 1. (a) Three dimensional view of multiplanar hexagonal nano-structures along with side views from two mutually perpendicular directions (b) Top view of multiplanar hexagonal nano-structures.

clearly identified and the top and bottom planes are symmetric with respect to the mid-plane). Thus there is a strong rationale to develop a generalized compact analytical model leading to closed-form and high fidelity expressions for characterizing the mechanical properties of hexagonal multiplanar nano-structures.

Figure 1 shows a generalized material nano-structure with hexagonal top view, wherein two different atoms are placed in different planes (such as MoS_2). There is a different class of materials which has same atoms in the hexagonal nano-structure, but placed in different planes (such as stanene). Other classes of materials have different atoms in the hexagonal nano-structure placed in a single plane (such as hBN) and same atom in the hexagonal nano-structure placed in a single plane (such as graphene). Thus based on nano-structural configurations, the materials with hexagonal nano-structure (top view) can be divided into four classes as presented in table 1. From structural point of view, the other classes of materials are basically special cases of the materials of Class D. Aim of the present work is to develop generalized closed form analytical formulae for the elastic moduli of such hexagonal multiplanar nano-structures that can be applicable for wide range of materials (Class A to Class D). This paper hereafter is organized as follows: analytical formulae for the elastic moduli of materials with multiplanar hexagonal nano-structures are derived in section 2; results and discussion on the proposed analytical approach is provided in section 3 along with validation of the developed formulae for four different materials belonging to four different classes (graphene, hBN, stanene and MoS_2); and finally conclusion and perspective of this work is presented in section 4.

2. Elastic properties of hexagonal nano-structures

Generalized closed-form analytical formulae for the elastic moduli of hexagonal multiplanar nano-structures are developed in this section that is applicable to all the materials from Class A to Class D (refer to table 1). The equivalent elastic properties of atomic bonds are described first, and thereby the closed-form expressions of elastic moduli for generalized multiplaner hexagonal nano-structures are derived. The approach for obtaining the equivalent elastic properties of atomic bonds is well-established in scientific literature [12, 14, 29]. Therefore, the main contributing of this work lies in the later part of this section concerning development of analytical formulae for elastic moduli of multiplanar hexagonal nano-structures. In this context, it can be noted that the mechanics of honeycomb-like structural form

Table 1. Structural-configuration based classification of hexagonal nano-materials.

Material type	Structural configuration	Description of nano-materials
Class A	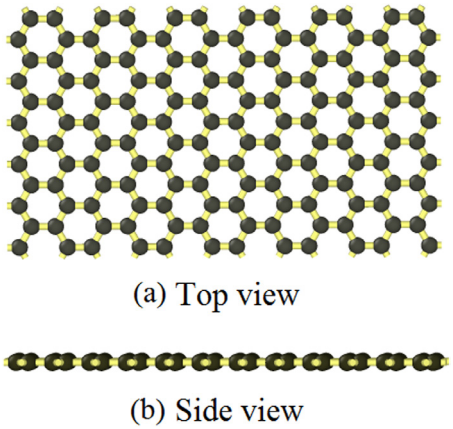 (a) Top view (b) Side view	*Characteristic property from structural point of view*: All the constituent atoms are same and they are in a single plane (e.g. graphene [4, 13])
Class B	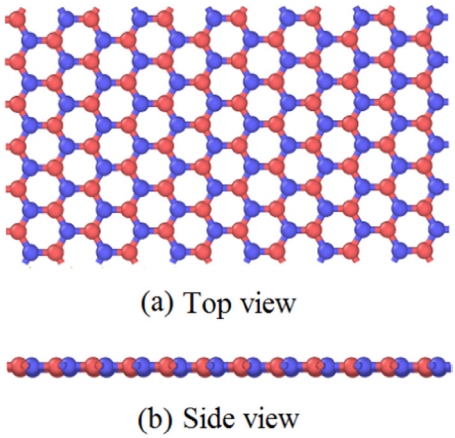 (a) Top view (b) Side view	*Characteristic property from structural point of view*: The constituent atoms are not same but they are in a single plane (e.g. hBN [15, 17], BCN [18])
Class C	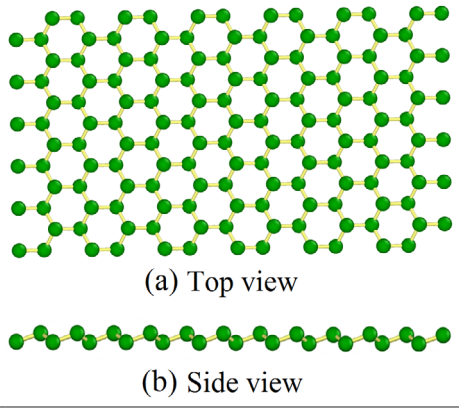 (a) Top view (b) Side view	*Characteristic property from structural point of view*: The constituent atoms are same but they are in two different planes (e.g. silicene [19, 20], germanene [21], phosphorene [22], stanene [20, 23], borophene [24])
Class D	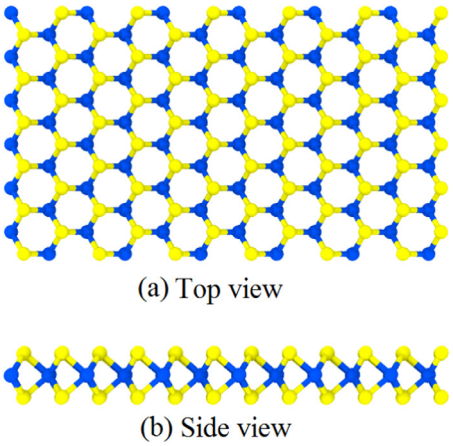 (a) Top view (b) Side view	*Characteristic property from structural point of view*: The constituent atoms are not same and they are in two different planes (e.g. MoS_2 [25], WS_2 [26], $MoSe_2$ [27], WSe_2 [26], $MoTe_2$ [28])

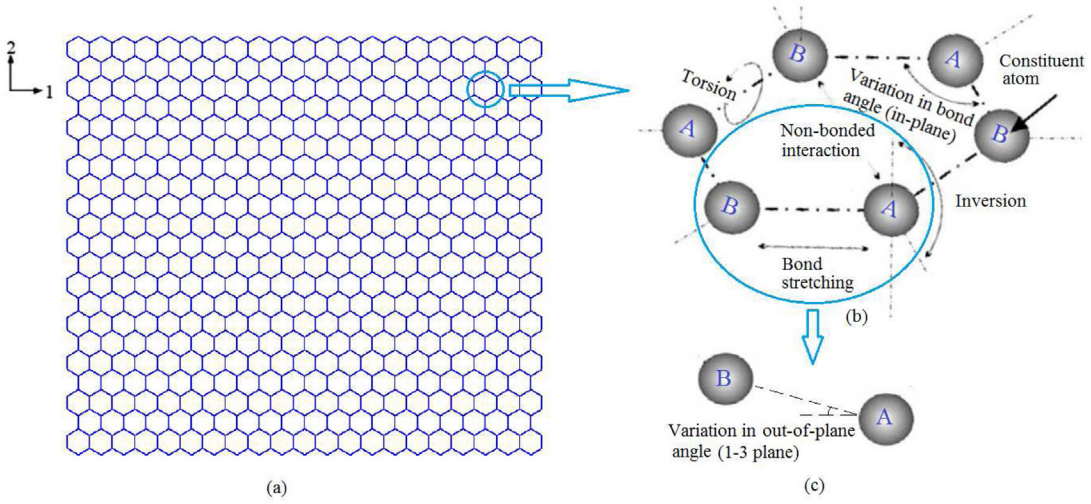

Figure 2. (a) Top view of hexagonal nano-structures (b) Bond structure in hexagonal nano-materials and associated energy components (c) Energy component associated with out-of-plane bending (Direction 1 and 2 are indicated in the figure. Direction 3 is perpendicular to the 1–2 plane.).

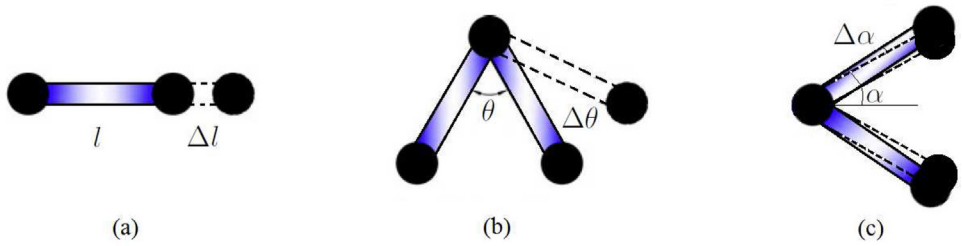

Figure 3. (a) Strain energy due to bond stretching (b) Strain energy due to in-plane angle variation (in 1–2 plane) (c) Strain energy due to out-of-plane angle variation (in 1–3 and 2–3 planes).

is investigated extensively in micro and macro scales based on principles of structural mechanics [30–34].

2.1. Equivalent elastic properties of atomic bonds

In nano-scale investigations concerning atomic level behaviour of materials, the total inter-atomic potential energy of a system can be expressed as the sum of different individual energy terms related to bonding and non-bonding interactions [12]. Total strain energy (E) of a nano-structure is the sum of energy contributions from bond stretching (E_s), bending (E_b), torsion (E_t) and energies associated with non-bonded terms (E_{nb}) such as the van der Waals attraction, the core repulsions and the coulombic energy (refer to figure 2).

$$E = E_s + E_b + E_t + E_{nb} \tag{1}$$

Among all the above mentioned energy components, effect of stretching and bending are predominant for small deformation of such nano-structures [14, 29]. However, for the hexagonal nano-structures where the atoms are not in a single plane (materials belonging to Class C and Class D as per table 1), the strain energy due to bending has two components. Typically the atoms stay in two different planes (/ two symmetric planes with respect to the middle layer) in such material structures and the total bending energy (E_b) consists of in-plane component (E_{bi}) and out-of-plane component (E_{bo}). Thus the total inter-atomic potential energy (E) can be expressed as

$$\begin{aligned} E &= E_s + E_b \\ &= E_s + E_{bi} + E_{bo} \\ &= \frac{1}{2}k_r(\Delta l)^2 + \frac{1}{2}k_\theta(\Delta\theta)^2 + \frac{1}{2}k_\theta(\Delta\alpha)^2 \end{aligned} \tag{2}$$

where Δl, $\Delta\theta$ and $\Delta\alpha$ denote the bond elongation, change in in-plane and out-of-plane angle respectively, as shown in figure 3. k_r and k_θ are the force constants associated with bond stretching and bending respectively. The first term in the above expression of total inter-atomic potential energy corresponds to strain energy due to stretching (E_s), while the second and third terms represent the strain energies due to in-plane (E_{bi}) and out-of-plane (E_{bo}) angle variations respectively.

The force constants (k_r and k_θ) of the bonds between two atoms can be expressed in terms of the member stiffness [35]. According to the standard theory of classical structural mechanics (refer to figure 4), strain energy of a uniform circular beam with cross-sectional area A, length l, Young's modulus E, and second moment of area I, under the application of a pure axial force N can be expressed as

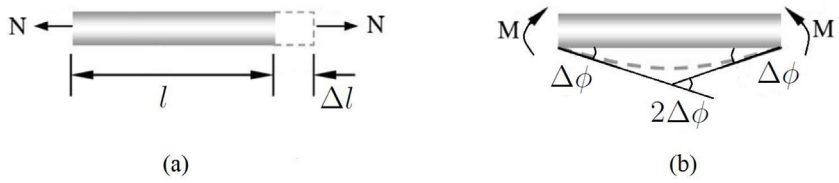

Figure 4. (a) A structural element subjected to pure tension (b) A structural element subjected to pure bending.

$$U_a = \frac{1}{2}\int_0^L \frac{N^2}{EA}\,\mathrm{d}l = \frac{1}{2}\frac{N^2 l}{EA} = \frac{1}{2}\frac{EA}{l}(\Delta l)^2 \quad (3)$$

The strain energies due to pure bending moment M can be written as

$$U_b = \frac{1}{2}\int_0^L \frac{M^2}{EI}\,\mathrm{d}l = \frac{1}{2}\frac{EI}{l}(2\Delta\phi)^2 \quad (4)$$

Comparing equation (3) with the expression for strain energy due to stretching (E_s) (refer equation (2)), it can be concluded that $K_r = \frac{EA}{l}$. For bending, it is reasonable to assume that $2\Delta\phi$ is equivalent to $\Delta\theta$ and $\Delta\alpha$ for in-plane and out-of-plane angle variations respectively (refer to figure 4(b)). Thus comparing equation (4) with the expressions for the strain energies due to in-plane (E_{bi}) and out-of-plane (E_{bo}) angle variations, the following relation can be obtained: $k_\theta = \frac{EI}{l}$. On the basis of the established relationship between molecular mechanics parameters (k_r and k_θ) and structural mechanics parameters (EA and EI), the effective elastic moduli of multiplanar hexagonal nano-structures are obtained in the following sections.

2.2. Young's modulus in direction-1 (E_1)

One hexagonal unit cell is considered to derive the expression for Young's moduli of the entire hexagonal periodic nano-structure as shown in figure 5. Because of structural symmetry, horizontal deformation of the unit cell can be obtained by analysing the member AB only. The total horizontal deformation of the member AB (horizontal deflection of one end of the member with respect to the other end) under the application of stress σ_1 has three components: axial deformation (δ_{aH}), bending deformation due to in-plane loading (δ_{bHi}) and bending deformation due to out-of-plane loading (δ_{bHo}).

$$\begin{aligned}\delta_{H11} &= \delta_{aH} + \delta_{bHi} + \delta_{bHo} \\ &= \frac{Hl\cos^2\psi\cos^2\alpha}{AE} + \frac{Hl^3\sin^2\psi}{12EI} \\ &\quad + \frac{Hl^3\cos^2\psi\sin^2\alpha}{12EI}\end{aligned} \quad (5)$$

where $A = \frac{\pi d^2}{4}$, $I = \frac{\pi d^4}{64}$ and $H = \sigma_1 tl(1+\sin\psi)\cos\alpha$. l and d represent the length and diameter of the member AB respectively. t is the thickness of single layer of such periodic structural form. The three parts of equation (5) are derived by considering the respective deformation components in direction-1. Figures 5(a) and (b) show the member AB using top-view and side-view respectively, wherein the horizontal load H acts at the node A in the 1–2 plane. Inclination angle of the member AB in the 1–2 plane and 1–3 plane are ψ and α respectively, as shown in figure 5(e). From figure 5(a) it can be understood that the horizontal force H has two components: $H\sin\psi$ (acting in a direction perpendicular to the member AB in the 1–2 plane) and $H\cos\psi$ (acting in a direction perpendicular to the force $H\sin\psi$ in the 1–2 plane). The $H\sin\psi$ component will cause a bending deflection Δ_{Hi}. The component of Δ_{Hi} in direction-1 is denoted as δ_{bHi} in equation (5). Using the standard formula of structural mechanics (bending deflection of one end of a beam with respect to the other end: $\delta = \frac{PL^3}{12EI}$, where L is the length of the beam, P is the applied point load across the beam length [36]) the component δ_{bHi} can be expressed as

$$\delta_{bHi} = \Delta_{Hi}\sin\psi = \frac{H\sin\psi l^3}{12EI}\sin\psi = \frac{Hl^3\sin^2\psi}{12EI} \quad (6)$$

The $H\cos\psi$ force can be resolved in two different components in the plane perpendicular to the 1–2 plane. The component $H\cos\psi\cos\alpha$ causes axial deformation of the member AB, while the other component $H\cos\psi\sin\alpha$ results in the bending deformation Δ_{Ho} (as indicated in figure 5(b)). The horizontal component of Δ_{Ho} in the 1–2 plane is denoted as δ_{bHo} in the equation (5). Thus we get

$$\begin{aligned}\delta_{bHo} &= \Delta_{Ho}\sin\alpha\cos\psi = \frac{H\cos\psi\sin\alpha l^3}{12EI}\sin\alpha\cos\psi \\ &= \frac{Hl^3\cos^2\psi\sin^2\alpha}{12EI}\end{aligned} \quad (7)$$

The horizontal axial deformation component in the 1–2 plane caused by the force $H\cos\psi\cos\alpha$ is denoted as δ_{aH} in the equation (5). Thus we get

$$\delta_{aH} = \frac{H\cos\psi\cos\alpha l}{AE}\cos\psi\cos\alpha = \frac{Hl\cos^2\psi\cos^2\alpha}{AE} \quad (8)$$

Using the relationship between molecular mechanics parameters (k_r and k_θ) and structural mechanics parameters (EA and EI), form equation (5), the expression for strain in direction-1 (due to loading in direction-1) can be written as

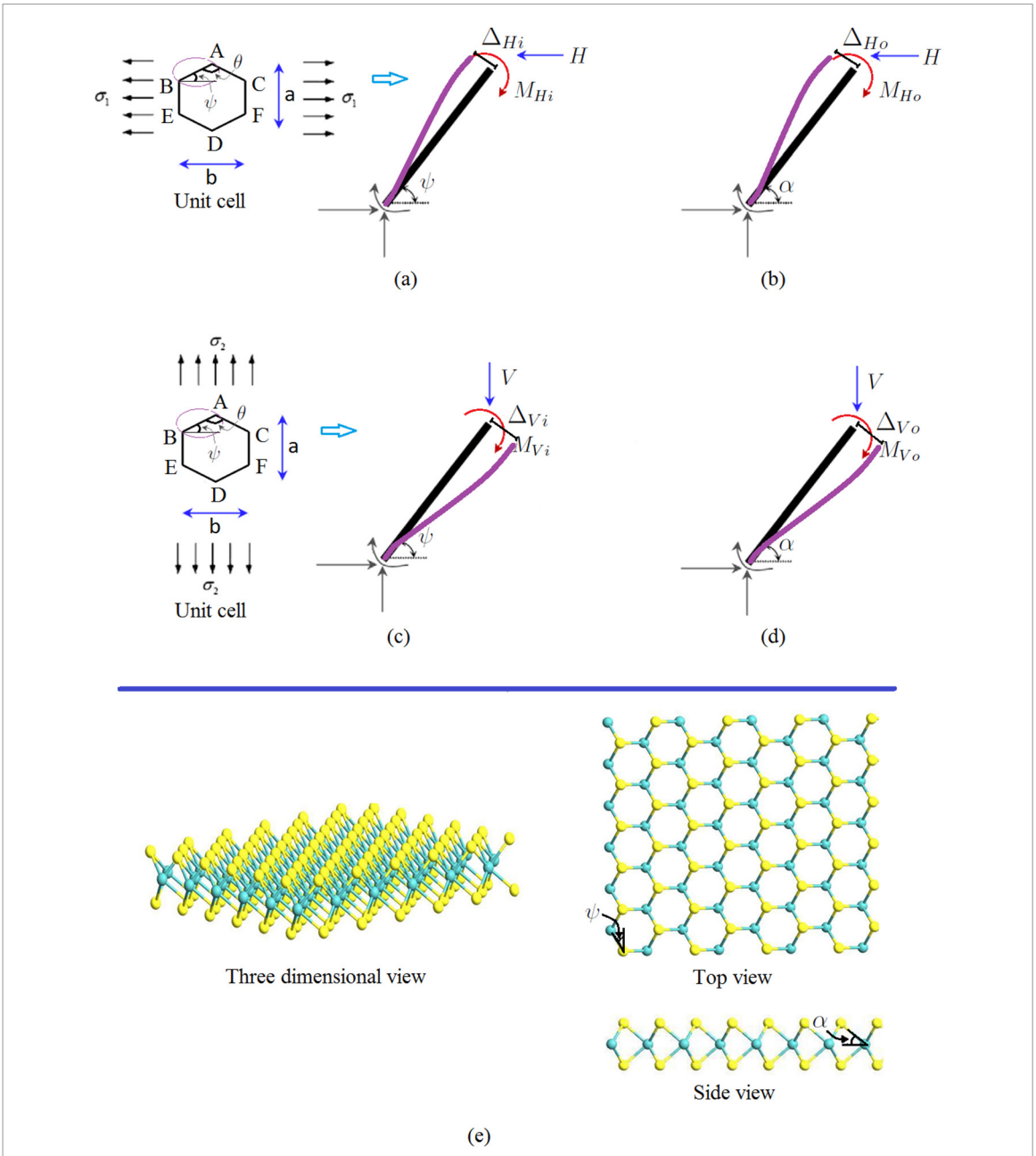

Figure 5. (a) Free body diagram of member AB for in-plane deformation under the application of horizontal force (b) Free body diagram of member AB for out-of-plane deformation under the application of horizontal force (c) Free body diagram of member AB for in-plane deformation under the application of vertical force (d) Free body diagram of member AB for out-of-plane deformation under the application of vertical force (e) Three dimensional view of a multiplanar hexagonal nanostructure along with top and side view indicating the in-plane angle (ψ) and out-of-plane angle (α).

$$\epsilon_{11} = \frac{\delta_{H11}}{l\cos\psi\cos\alpha} = \frac{\sigma_1 tl(1+\sin\psi)}{l\cos\psi}\left(\frac{l^2}{12k_\theta}(\sin^2\psi+\cos^2\psi\sin^2\alpha) + \frac{\cos^2\psi\cos^2\alpha}{k_r}\right) \tag{9}$$

On the basis of the basic definition of Young's modulus ($E_1 = \frac{\sigma_1}{\epsilon_{11}}$), the closed-form expression for Young's modulus in direction-1 can be obtained as

$$E_1 = \frac{\cos\psi}{t(1+\sin\psi)\left(\frac{l^2}{12k_\theta}(\sin^2\psi+\cos^2\psi\sin^2\alpha)+\frac{\cos^2\psi\cos^2\alpha}{k_r}\right)} \tag{10}$$

In the above expression $\psi = 90^\circ - \frac{\theta}{2}$, where θ is the bond angle as shown in figure 5.

2.3. Young's modulus in direction-2 (E_2)

Total vertical deformation of the unit cell under the application of σ_2 is consisted of the deformation of member AB (δ_{V1}) and member BE (δ_{V2}) in direction-2.

Deflection of joint A in direction-2 with respect to joint B has three components: axial deformation (δ_{aV1}), bending deformation due to in-plane loading (δ_{bV1i}) and bending deformation due to out-of-plane loading (δ_{bV1o}).

$$\begin{aligned}\delta_{V1} &= \delta_{aV1} + \delta_{bV1i} + \delta_{bV1o} \\ &= \frac{Vl\sin^2\psi\cos^2\alpha}{AE} + \frac{Vl^3\cos^2\psi}{12EI} \\ &\quad + \frac{Vl^3\sin^2\psi\sin^2\alpha}{12EI}\end{aligned} \tag{11}$$

where $V = \sigma_2 tl\cos\psi\cos\alpha$. As the member BE is parallel to the 2-3 plane, deflection of joint B with respect to the joint E has two components: axial deformation (δ_{aV2}) and bending deformation due to out-of-plane loading (δ_{bV2o}). It can be noted that the force acting on the member BE is $2V$ as there are similar unit cells adjacent to the one being analysed.

$$\begin{aligned}\delta_{V2} &= \delta_{aV2} + \delta_{bV2o} \\ &= \frac{2Vl\cos^2\alpha}{AE} + \frac{2Vl^3\sin^2\alpha}{12EI}\end{aligned} \tag{12}$$

Replacing the expressions of V, A, I, AE and EI, the total deformation in direction-2 can be obtained from equations (11) and (12) as

$$\begin{aligned}\delta_{V22} &= \delta_{V1} + \delta_{V2} \\ &= \sigma_2 tl\cos\psi\cos\alpha \\ &\quad \times\left(\frac{l^2}{12k_\theta}(\cos^2\psi + \sin^2\psi\sin^2\alpha + 2\sin^2\alpha)\right. \\ &\quad \left. + \frac{\cos^2\alpha}{k_r}(\sin^2\psi + 2)\right)\end{aligned} \tag{13}$$

From equation (13), the strain in direction-2 (due to loading in direction-2) can be expresses as

$$\begin{aligned}\epsilon_{22} &= \frac{\delta_{V22}}{(l + l\sin\psi)\cos\alpha} \\ &= \frac{\sigma_2 t\cos\psi}{1+\sin\psi} \\ &\quad \times\left(\frac{l^2}{12k_\theta}(\cos^2\psi + \sin^2\psi\sin^2\alpha + 2\sin^2\alpha)\right. \\ &\quad \left. + \frac{\cos^2\alpha}{k_r}(\sin^2\psi + 2)\right)\end{aligned} \tag{14}$$

On the basis of the basic definition of Young's modulus ($E_2 = \frac{\sigma_2}{\epsilon_{22}}$), the closed-form expression for Young's modulus in direction-2 can be obtained as

$$E_2 = \frac{1+\sin\psi}{t\cos\psi\left(\frac{l^2}{12k_\theta}(\cos^2\psi + \sin^2\psi\sin^2\alpha + 2\sin^2\alpha) + \frac{\cos^2\alpha}{k_r}(\sin^2\psi + 2)\right)} \tag{15}$$

In the above expression $\psi = 90^\circ - \frac{\theta}{2}$, where θ is the bond angle as shown in figure 5. Thus the Young's moduli of a material with hexagonal nano-structure can be predicted using the closed-form formulae (equations (10) and (15)) from molecular mechanics parameters (k_r and k_θ), bond length (l), bond angle (θ) and out-of-plane angle (α), which are available in the molecular mechanics literature.

2.4. Poisson's ratio ν_{12}

Poisson's ratio for the loading direction-1 (ν_{12}) can be obtained as

$$\nu_{12} = -\frac{\epsilon_{12}}{\epsilon_{11}} \tag{16}$$

where ϵ_{12} and ϵ_{11} are the strains in direction-2 and direction-1 respectively due to loading in direction-1. The expression for ϵ_{11} is given in equation (9). Derivation for the expression of ϵ_{12} is provided next. The deformation in direction-2 due to loading in direction-1 can be obtained by considering one hexagonal unit cell as shown in figure 5. Because of structural symmetry, deformation in direction-2 of the unit cell due to loading in direction-1 can be obtained by analysing the member AB only. The total deformation in direction-2 of the member AB (deflection in direction-2 of one end of the member with respect to the other end) under the application of stress σ_1 has two components: bending deformation due to in-plane loading (δ_{bVi1}) and bending deformation due to out-of-plane loading (δ_{bVo1}).

$$\begin{aligned}\delta_{H12} &= \delta_{bVi1} + \delta_{bVo1} \\ &= -\frac{Hl^3\sin\psi\cos\psi}{12EI} + \frac{Hl^3\sin\psi\cos\psi\sin^2\alpha}{12EI} \\ &= -\frac{Hl^3\sin\psi\cos\psi\cos^2\alpha}{12EI}\end{aligned} \tag{17}$$

Using the relationship between molecular mechanics parameter k_θ and structural mechanics parameter EI, form equation (17), the expression for strain in direction-2 (due to loading in direction-1) can be written as

$$\begin{aligned}\epsilon_{12} &= \frac{\delta_{H12}}{(l + l\sin\psi)\cos\alpha} \\ &= -\frac{Hl\sin\psi\cos\psi\cos\alpha}{12k_\theta(1+\sin\psi)}\end{aligned} \tag{18}$$

On the basis of the basic definition of ν_{12} as shown in equation (16), the closed-form expression of Poisson's ratio for the loading direction-1 can be obtained as

$$\nu_{12} = \frac{\sin\psi\cos^2\psi\cos^2\alpha l^2}{12k_\theta(1+\sin\psi)\left(\frac{l^2}{12k_\theta}(\sin^2\psi + \cos^2\psi\sin^2\alpha) + \frac{\cos^2\psi\cos^2\alpha}{k_r}\right)} \tag{19}$$

In the above expression $\psi = 90^\circ - \frac{\theta}{2}$, where θ is the bond angle as shown in figure 5.

2.5. Poisson's ratio ν_{21}

Poisson's ratio for the loading direction-2 (ν_{21}) can be obtained as

$$\nu_{21} = -\frac{\epsilon_{21}}{\epsilon_{22}} \tag{20}$$

where ϵ_{21} and ϵ_{22} are the strains in direction-1 and direction-2 respectively due to loading in direction-2. The expression for ϵ_{22} is given in equation (14). Derivation for the expression of ϵ_{21} is provided next. The deformation in direction-1 due to loading in direction-2 can be obtained by considering one hexagonal unit cell as shown in equation (5). Because of structural symmetry, deformation in direction-1 of the unit cell due to loading in direction-2 can be obtained by analysing the member AB only. The total deformation in direction-1 of the member AB (deflection in direction-1 of one end of the member with respect to the other end) under the application of stress σ_2 has two components: bending deformation due to in-plane loading (δ_{bHi2}) and bending deformation due to out-of-plane loading (δ_{bHo2}).

$$\begin{aligned}\delta_{H21} &= \delta_{\mathrm{bHi2}} + \delta_{\mathrm{bHo2}} \\ &= -\frac{Vl^3 \sin\psi\cos\psi}{12EI} + \frac{Vl^3 \sin\psi\cos\psi\sin^2\alpha}{12EI} \\ &= -\frac{Vl^3 \sin\psi\cos\psi\cos^2\alpha}{12EI}\end{aligned} \tag{21}$$

Using the relationship between molecular mechanics parameter k_θ and structural mechanics parameter EI, form equation (21), the expression for strain in direction-1 (due to loading in direction-2) can be written as

$$\begin{aligned}\epsilon_{21} &= \frac{\delta_{H21}}{l\cos\psi\cos\alpha} \\ &= -\frac{Vl\sin\psi\cos\alpha}{12k_\theta}\end{aligned} \tag{22}$$

On the basis of the basic definition of ν_{21} as shown in equation (20), the closed-form expression of Poisson's ratio for the loading direction-2 can be obtained as

$$\nu_{21} = \frac{\sin\psi(1+\sin\psi)\cos^2\alpha l^2}{12k_\theta\left(\frac{l^2}{12k_\theta}(\cos^2\psi + \sin^2\psi\sin^2\alpha + 2\sin^2\alpha) + \frac{\cos^2\alpha}{k_r}(\sin^2\psi + 2)\right)} \tag{23}$$

In the above expression $\psi = 90^\circ - \frac{\theta}{2}$, where θ is the bond angle as shown in figure 5.

2.6. Remark 1: reciprocal theorem

From the equations (10), (15), (19) and (23), it can be noticed that the reciprocal theorem is obeyed for multiplanar hexagonal nanostructures

$$E_1\nu_{21} = E_2\nu_{12} = \frac{\sin\psi\cos\psi\cos^2\alpha l^2\left(\frac{l^2}{12k_\theta}(\sin^2\psi + \cos^2\psi\sin^2\alpha) + \frac{\cos^2\psi\cos^2\alpha}{k_r}\right)^{-1}}{12k_\theta t\left(\frac{l^2}{12k_\theta}(\cos^2\psi + \sin^2\psi\sin^2\alpha + 2\sin^2\alpha) + \frac{\cos^2\alpha}{k_r}(\sin^2\psi + 2)\right)} \tag{24}$$

The above equation implies that only (any) three of the four elastic moduli E_1, E_2, ν_{12} and ν_{21} are independent.

2.7. Remark 2: non-dimensionalization

The physics based analytical formulae developed in this article are capable of providing an in-depth understanding of the behaviour of multiplanar hexagonal nano-structures. Non-dimesional quantities in physical systems can cater to an insight for wide range of nano-scale materials. The expressions for the two Young's moduli (as presented in equations (10) and (15)) and the two Poisson's ratios (as presented in equations (19) and (23)) can be rewritten in terms of non-dimensional parameters as

$$\tilde{E}_1 = \frac{\cos\psi}{(1+\sin\psi)(\lambda(\sin^2\psi + \cos^2\psi\sin^2\alpha) + \cos^2\psi\cos^2\alpha)} \tag{25}$$

$$E_2 = \frac{1+\sin\psi}{\cos\psi(\lambda(\cos^2\psi + \sin^2\psi\sin^2\alpha + 2\sin^2\alpha) + \cos^2\alpha(\sin^2\psi + 2))} \tag{26}$$

$$\tilde{\nu}_{12} = \frac{\sin\psi\cos^2\psi\cos^2\alpha\lambda}{(1+\sin\psi)(\lambda(\sin^2\psi + \cos^2\psi\sin^2\alpha) + \cos^2\psi\cos^2\alpha)} \tag{27}$$

$$\nu_{21} = \frac{\sin\psi(1+\sin\psi)\cos^2\alpha\lambda}{(\lambda(\cos^2\psi + \sin^2\psi\sin^2\alpha + 2\sin^2\alpha) + \cos^2\alpha(\sin^2\psi + 2))} \tag{28}$$

where $\lambda\left(=\frac{l^2}{12}\frac{k_r}{k_\theta}\right)$ is a non-dimensional aspect ratio measure of the bonds that is found to vary in the range of 0.4–2.8 for common materials with hexagonal nano-structures. It is interesting to notice that λ reduces to $\frac{4}{3}\left(\frac{l}{d}\right)^2$ using the definition of k_r and k_θ, where l and d are

Table 2. Results for Young's moduli of single layer materials with four different classes of nano-structure as described in table 1 (results are presented as $\bar{E}_1 = E_1 \times t$ and $\bar{E}_2 = E_2 \times t$, where t is the single layer thickness of a particular nano-material).

Material	Present results (TPa nm)	Reference results from literature ($\bar{E}_1 = \bar{E}_2$) (TPa nm)
Graphene (Class A)	$\bar{E}_1 = 0.3542$ $\bar{E}_2 = 0.3542$	Experimental: 0.34 ± 0.034 [38], 0.272–0.306 [39] *Ab initio*: 0.350 [40], 0.357 [10], 0.377 [41], 0.364 [42] Molecular dynamics: 0.357 [43], 0.343 ± 0.01 [44] Molecular mechanics: 0.354 [14], 0.3604 [12]
hBN (Class B)	$\bar{E}_1 = 0.2659$ $\bar{E}_2 = 0.2659$	Experimental: 0.251 ± 0.015 [47] *Ab initio*: 0.271 [40], 0.272 [48] Molecular dynamics: 0.236 [49], 0.278 [50] Molecular Mechanics: 0.269 [51], 0.322 [52]
Stanene (Class C)	$\bar{E}_1 = 0.0545$ $\bar{E}_2 = 0.0643$	Experimental: — *Ab initio*: 0.0528 [45] Molecular dynamics: — Molecular Mechanics: —
MoS_2 (Class D)	$\bar{E}_1 = 0.1073$ $\bar{E}_2 = 0.2141$	Experimental: 0.211 ± 0.012 [53], 0.1629 ± 0.0603 [46] *Ab initio*: 0.141 [54], 0.262 [55] Molecular dynamics: 0.150 [56] Molecular mechanics: —

the bond length and bond diameter respectively. Thus the parameter λ is a measure of the aspect ratio of the bonds in hexagonal nano-structure. $E_1 = \frac{E_1 t}{k_r}$ and $E_2 = \frac{E_2 t}{k_r}$ are non-dimensional representation of the Young's moduli. ν_{12} $(= \nu_{12})$ and ν_{21} $(= \nu_{21})$ are the non-dimensional Poisson's ratios. Thus it is interesting to notice that the non-dimensional elastic moduli depend on the aspect ratio of the bond, in-plane angle and out-of-plane angles only. Results are presented in section 3 considering the non-dimensional quantities for in-depth mechanical characterization of hexagonal nano-structures.

2.8. Remark 3: special cases

For the hexagonal nano-structures belonging to Class A and Class B, $\alpha = 0$. Thus equations (10) and (15) for the materials of Class A and Class B reduce to

$$E_1 = \frac{\cos\psi}{t(1+\sin\psi)\left(\frac{l^2}{12k_\theta}\sin^2\psi + \frac{\cos^2\psi}{k_r}\right)} \tag{29}$$

$$E_2 = \frac{1+\sin\psi}{t\cos\psi\left(\frac{l^2}{12k_\theta}\cos^2\psi + \frac{(\sin^2\psi+2)}{k_r}\right)} \tag{30}$$

However, for regular hexagonal nano-structures (such as graphene), the bond angle (θ) is120°. Thus replacing $\psi = 30°$, the equations (29) and (30) yield to

$$E_1 = E_2 = \frac{4\sqrt{3}\,k_r k_\theta}{t\left(\frac{k_r l^2}{4} + 9k_\theta\right)} \tag{31}$$

The above expression matches with the formula provided by Shokrieh and Rafiee [14] for graphene.

Similarly, for the hexagonal nano-structures belonging to Class A and Class B, the Poisson's ratios can be expressed as (substituting $\alpha = 0$ in equations (19) and (23))

$$\nu_{12} = \frac{\sin\psi\cos^2\psi l^2}{12k_\theta(1+\sin\psi)\left(\frac{l^2}{12k_\theta}\sin^2\psi + \frac{\cos^2\psi}{k_r}\right)} \tag{32}$$

$$\nu_{21} = \frac{\sin\psi(1+\sin\psi)l^2}{12k_\theta\left(\frac{l^2}{12k_\theta}\cos^2\psi + \frac{(\sin^2\psi+2)}{k_r}\right)} \tag{33}$$

However, for regular hexagonal nano-structures (such as graphene), the bond angle (θ) is120°. Thus replacing $\psi = 30°$, the equations (32) and (33) yield to

$$\nu_{12} = \nu_{21} = \frac{1}{1+\frac{36k_\theta}{k_r l^2}} \tag{34}$$

It can be noted that the analytical expressions of Poisson's ratios, even for graphene-like hexagonal structures, are first provided in equation (34) that can be applicable to the materials of Class A and Class B.

3. Results and discussion

Four different materials with hexagonal nano-structures are considered (graphene, hBN, stanene and MoS_2) that belong to four different classes as categorized in table 1. To validate the analytical formulae of elastic moduli derived in the preceding section, the results are compared with previous studies reported in scientific literature (experimental, *ab initio*, molecular dynamics and molecular mechanics, as available). The proposed expressions for elastic moduli are generalized in nature and they can be applicable for wide range of materials with hexagonal nano-structural forms by providing respective structural parameters as input. Comparative results for the two Young's moduli are presented in table 2 as $\bar{E}_1 = E_1 \times t$ and $\bar{E}_2 = E_2 \times t$ (tensile rigidity), where t is the single layer thickness [12, 15]. Thus the values of Young's moduli (E_1 and E_2

Table 3. Results for Poisson's ratios of single layer materials with four different classes of nano-structure as described in table 1.

Material	Present results	Reference results from literature
Graphene (Class A)	$\nu_{12} = 0.2942$ $\nu_{21} = 0.2942$	Experimental: 0.165 [57] *Ab initio*: 0.12–0.16 [42], 0.186 [10], 0.34 [58] Molecular dynamics: 0.17 [43], 0.41 [59] Molecular mechanics: 0.11–0.12 [60], 0.195 [61], 0.653–0.848 [13], 1.129–1.1441 [62]
hBN (Class B)	$\nu_{12} = 0.2901$ $\nu_{21} = 0.2901$	Experimental: — *Ab initio*: 0.2–0.3 [63], 0.211 [40], 0.2–0.24 [63], 0.13–0.16 [64] Molecular Dynamics: — Molecular mechanics: 0.384–0.389 [15], 0.400–0.405 [15], 0.384–0.389 [15], 0.211 [15], 0.053 [15], 0.2–0.4 [65]
Stanene (Class C)	$\nu_{12} = 0.1394$ $\nu_{21} = 0.1645$	Experimental: — *Ab initio*: — Molecular Dynamics: — Molecular Mechanics: —
MoS_2 (Class D)	$\nu_{12} = 0.0690$ $\nu_{21} = 0.1376$	Experimental: — *Ab initio*: 0.21 [66] Molecular dynamics: 0.29 [56] Molecular Mechanics: —

in TPa) can be obtained by dividing the presented values ($\bar{E}_1$ and $\bar{E}_2$ with unit TPa nm) by the respective single layer thickness (t in nm). Single layer thickness of the four considered materials are indicated in the following paragraphs. Comparative results for the two Poisson's ratio are presented in table 3. Good agreement between the results obtained using the derived closed-form formulae and the results from scientific literature for all the four classes of material corroborates the validity of the proposed analytical approach.

Graphene belongs to the Class A according to structural configuration, wherein all the atoms are carbon and they are in a single plane. The molecular mechanics parameters k_r and k_θ can be obtained from literature using AMBER force filed [37] as $k_r = 938$ kcal mol^{-1}nm $^{-2}$= 6.52×10^{-7} Nnm^{-1} and $k_\theta = 126$ kcal mol^{-1}rad $^{-2}$= 8.76×10^{-10} Nnm rad^{-2}. The out-of-plane angle for graphene is $\alpha = 0$ and the bond angle is $\theta = 120°$ (i.e. $\psi = 30°$), while bond length and thickness of single layer graphene can be obtained from literature as 0.142 nm and 0.34 nm respectively [13]. The value of Young's moduli obtained using the proposed expressions are: $E_1 = E_2 = 1.0419$ TPa, which is quite in good agreement with available literature [10, 12–14, 38–44] (refer to table 2).

Hexagonal boron nitride (hBN) belongs to the Class B according to structural configuration, wherein two different atoms B and N form the material structure but they are in a single plane. The molecular mechanics parameters k_r and k_θ can be obtained from literature using DREIDING force model [67] as $k_r = 4.865 \times 10^{-7}$ Nnm^{-1} and $k_\theta = 6.952 \times 10^{-10}$ Nnm rad^{-2} [17]. The out-of-plane angle for hBN is $\alpha = 0$ and the bond angle is $\theta = 120°$ (i.e. $\psi = 30°$), while bond length and thickness of single layer hBN can be obtained from literature as 0.145 nm and 0.098 nm respectively [15]. The value of tensile rigidity (Young's modulus multiplied by thickness) obtained using the proposed expressions are: $\bar{E_1} = \bar{E_2} = 0.2659$ TPa nm, which are quite in good agreement with available literature [15, 40, 47–49, 51, 52, 64, 65, 68] (refer to table 2).

Stanene belongs to the Class C according to structural configuration, wherein all the atoms are Sn but they are in two different planes. The molecular mechanics parameters k_r and k_θ can be obtained from literature as $k_r = 0.85 \times 10^{-7}$ Nnm^{-1} and $k_\theta = 1.121 \times 10^{-9}$ Nnm rad^{-2} [45, 69]. The out-of-plane angle for stanene is $\alpha = 17.5°$ and the bond angle is $\theta = 109°$ (i.e. $\psi = 35.5°$), while bond length and thickness of single layer stanene can be obtained from literature as 0.283 nm and 0.086 nm respectively [45, 69–71]. Published studies concerning the Young's moduli of stanene is very scarce in scientific literature. Thus the presented values of Young's moduli in this paper can serve as future references. The in-plane stiffness of stanene reported by Modarresi *et al.* [45] is 0.04 TPa nm irrespective of any direction. However, it should be noted that the in-plane stiffness of a material having hexagonal nano-structure depends on the direction of applied stress according to its definition. In-plane stiffness of a material can be defined as follows: $F = \frac{EA}{L}\Delta L = k\Delta L$, where $k\left(=\frac{EA}{L}\right)$ is the in-plane stiffness. Here L and ΔL represent the length of the material along the direction of applied stress and elongation in that direction respectively. E denotes the Young's modulus along the direction of applied stress. A is the cross-sectional area for applied stress. Thus, considering the unit cell shown in figure 5, the in-plane stiffness in direction-1 and direction-2 (refer to figure 2 for directions) can be expressed as: $k_1 = E_1 t\left(\frac{a}{b}\right) = \bar{E}_1\left(\frac{a}{b}\right)$ and $k_2 = E_2 t\left(\frac{b}{a}\right) = \bar{E}_2\left(\frac{b}{a}\right)$ respectively. For stanene the parameters a and b can be calculated from the bond length and in-plane angle as: $a = 0.61$ nm and $b = 0.46$ nm. The value of Young's moduli from the proposed

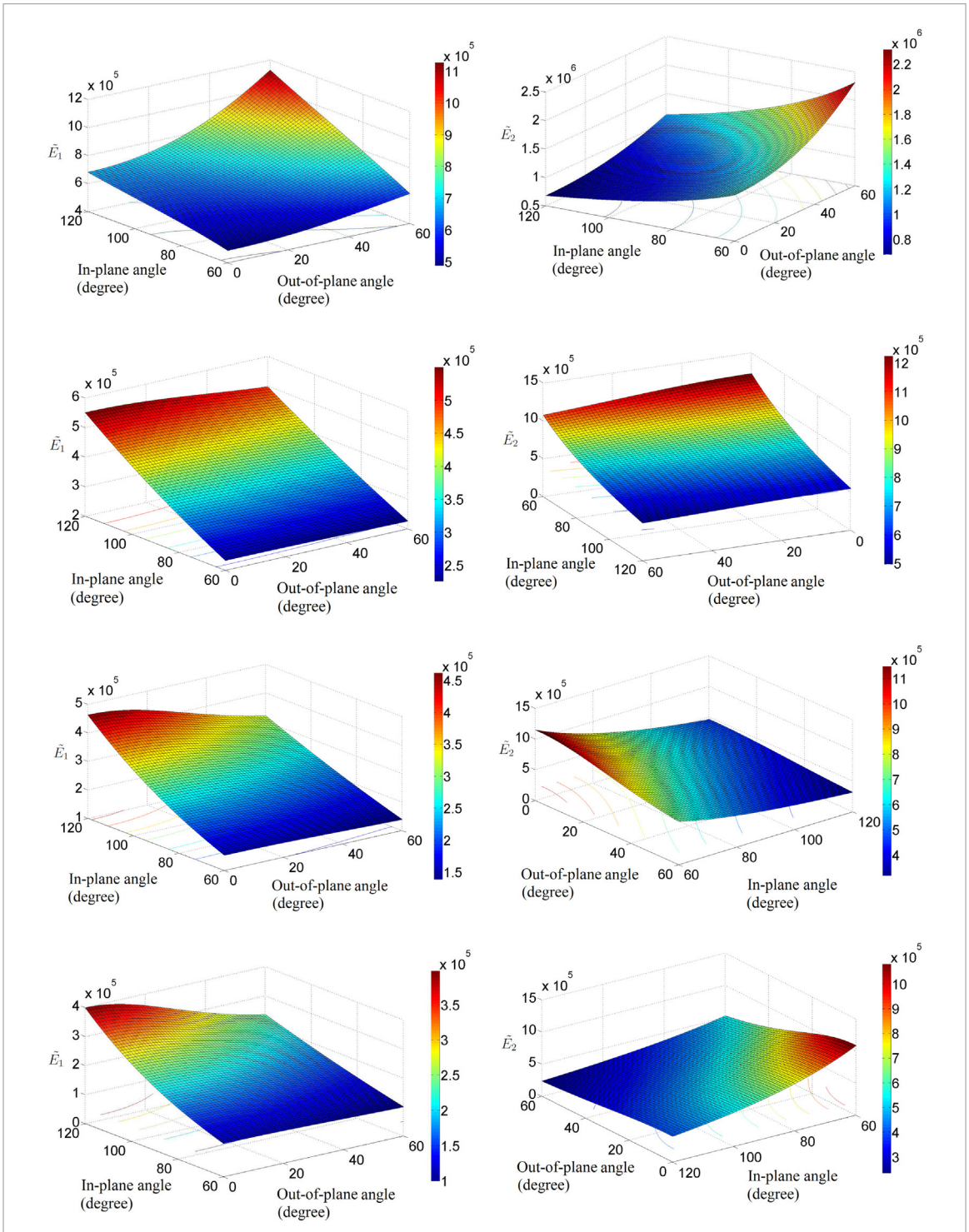

Figure 6. Variation of Young's moduli with in-plane bond angle (θ) and out-of-plane angle (α). Here $\lambda = \frac{l^2 k_r}{12 k_\theta}$, $E_1 = \frac{E_1 t}{k_r}$, $E_2 = \frac{E_2 t}{k_r}$, where l and t are the bond length and single layer thickness.

expressions are: $E_1 = 0.3166$ TPa and $E_2 = 0.3736$ TPa, thereby the tensile rigidity (Young's modulus multiplied by thickness) in the two directions can be obtained as: $\bar{E}_1 = 0.0545$ TPa nm and $\bar{E}_2 = 0.0643$ TPa nm. As per the above discussion, the in-plane stiffness can be obtained from the proposed expressions as: $k_1 = 0.0723$ TPa nm and $k_2 = 0.0484$ TPa nm. Thus the in-plane stiffness in direction-2 calculated using the present formulae is quite close to the values provided by Modarresi *et al* [45], wherein the results are reported presumably considering the direction-2 (refer to table 2).

Molybdenum disulfide (MoS_2) belongs to the Class D according to structural configuration, wherein two different atoms Mo and S form the material structure and they are in two different planes. The molecular mechanics parameters k_r and k_θ can be obtained from literature as $k_r = 1.646 \times 10^{-7}$ Nnm^{-1} and $k_\theta = 1.677 \times 10^{-9}$ Nnm rad^{-2}, while the out-of-plane angle, bond angle, bond length and thickness of single layer MoS_2 are $\alpha = 48.15°, \theta = 82.92°$ (i.e. $\psi = 48.54°$), 0.242 nm and 0.6033 nm respectively [25, 72–76]. The value of tensile rigidity (Young's modulus multiplied

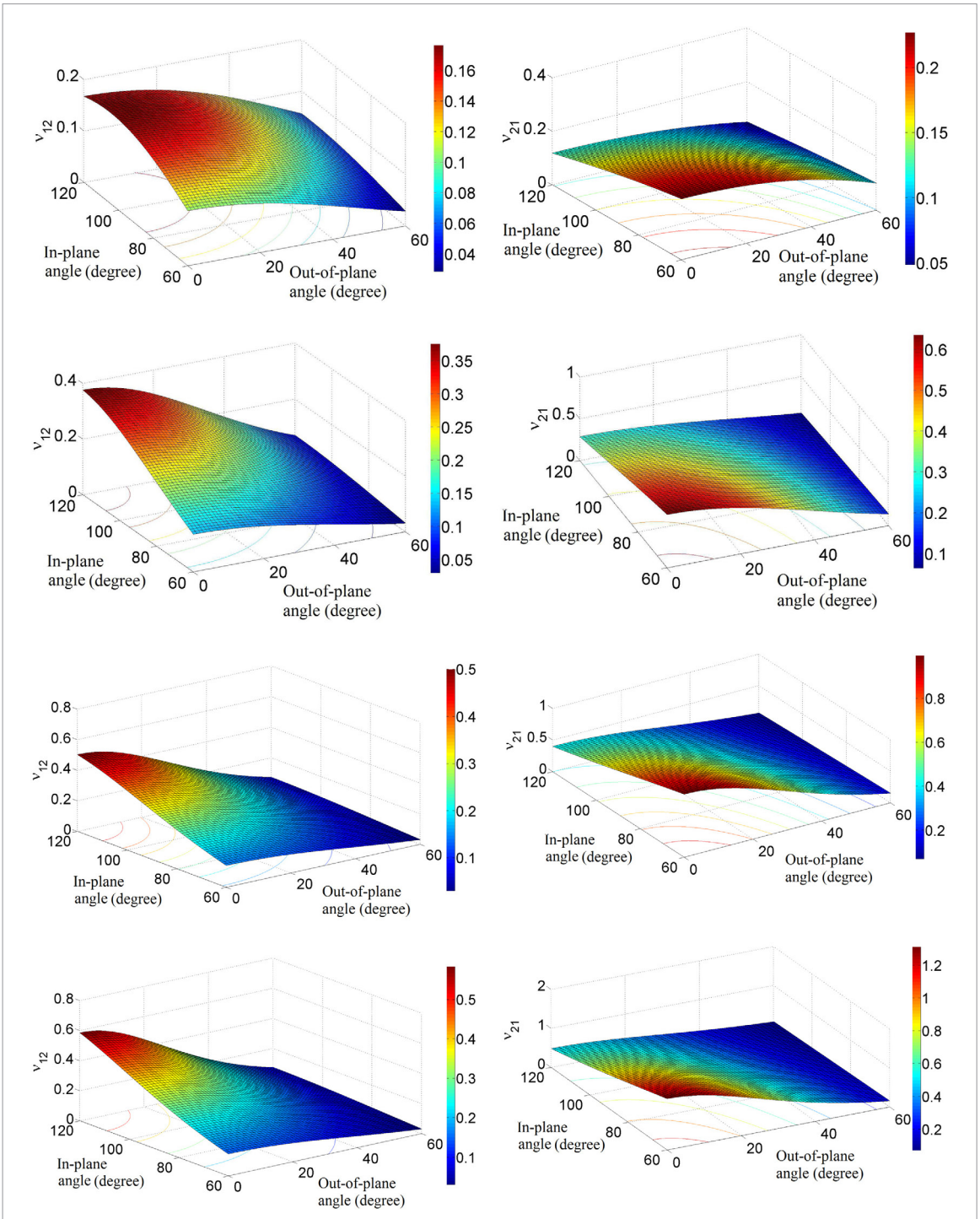

Figure 7. Variation of Poisson's ratios ($\nu_{12} = \nu_{12}$ and $\nu_{21} = \nu_{21}$) with in-plane bond angle (θ), out-of-plane angle (α) and $\lambda\,(=\frac{l^2 k_r}{12 k_\theta})$.

by thickness) obtained using the proposed expressions are: $\bar{E}_1 = 0.1073$ and $\bar{E}_2 = 0.2141$ TPa nm, which are quite in good agreement with available literature [46, 53–56, 77] (refer to table 2).

The results for Poisson's ratios obtained from the proposed analytical formulae are provided in table 3 along with reference values from literature. The reported values in literature for graphene and hBN show wide range of variability, while the reference values of Poisson's ratios for stanene and MoS_2 are very scarce in the scientific literature. The results obtained using the proposed formulae agree well with majority of the reported values for Poisson's ratios. However, it is noteworthy that for graphene and hBN $\nu_{12} = \nu_{21}$, while for stanene and MoS_2 $\nu_{12} < \nu_{21}$. The reciprocal theorem is satisfied perfectly for all the four classes of materials.

The physics based analytical formulae presented in this article are capable of providing a thorough insight regarding the behaviour of multiplanar hexagonal nano-structures representing wide range of materials. Variations of the two non-dimensional Young's moduli (E_1 and E_2) and the two Poisson's ratios with in-plane and out-of-plane angles (θ and α) for different

values of the aspect ratio measure (λ) are presented in figure 6 and 7 using the non-dimensional parameters as described in section 2.7. The aspect ratio measure of the bonds (λ) varies in the range of 0.4 to 2.8 for common materials with hexagonal nano-structures (specifically in case of the four considered materials: $\lambda = 1.2507, 2.495, 0.5061, 0.479$ for graphene, hBN, stanene and MoS_2 respectively). It is observed that the sensitivity of the out-of-plane angle is lesser compared to in-plane angle for both the non-dimensional Young's moduli on the basis of the slopes in two perpendicular directions of the surface plots. Such plots can readily provide the idea about the elastic moduli of any material with hexagonal nano-structure in a comprehensive manner; exact values of the elastic moduli can be easily obtained using the proposed computationally efficient closed-form formulae.

It is interesting to notice from the presented results that for graphene and hBN, $E_1 = E_2$ and $\nu_{12} = \nu_{21}$, while for stanene and MoS_2, $E_1 < E_2$ and $\nu_{12} < \nu_{21}$. In a broader sense, materials having regular hexagonal nano-structures with $\theta = 120^\circ$ and $\alpha = 0^\circ$ (Class A and Class B) have equal value of elastic modulus in two perpendicular directions. However, for materials belonging to Class C and Class D, the elastic modulus for direction-2 is more than that of direction-1, even though the difference is not significant. Similar trend is found to be reported for MoS_2 by Li [78]. A major contribution of this article is development of the generalized closed-form formulae for hexagonal nano-structures having the atoms in multiple planes. Mechanical properties such as Young's moduli and Poisson's ratios are of utmost importance for accessing the viability of their use in various applications of nanoelectromechanical systems. The formulae for elastic moduli presented in this article can serve as an efficient reference for any nano-scale material having hexagonal structural form.

4. Conclusion

Generalized closed-form analytical formulae for the elastic moduli of hexagonal multiplanar nano-structures are developed in this article. From the nano-structural point of view, the materails having hexagonal structural forms are categorized in four different classes. The proposed analytical formulae are applicable to all the classes of material. Four different materials belonging to the four different classes (graphene, hBN, stanene and MoS_2) are considered to present results based on the analytical approach. Good agreement in the results obtained from the derived analytical expressions and scientific literature corroborates the validity of the proposed formulae. The physics based analytical formulae developed in this article are capable of providing a comprehensive in-depth insight regarding the behaviour of such multiplanar hexagonal nano-structures. The effect of variation in in-plane and out-of-plane angles to the elastic moduli of materials are investigated using the closed-form formulae based on non-dimensional parameters. An attractive feature of the analytical approach is that it is computationally efficient and easy to implement, yet yields accurate results. As the proposed formulae are general in nature and applicable to wide range of materials with hexagonal nano-structures, the present article can take a crucial role for characterizing the material properties in future nano-materials development.

Acknowledgments

TM acknowledges the financial support from Swansea University through the award of Zienkiewicz Scholarship. SA acknowledges the financial support from The Royal Society of London through the Wolfson Research Merit award.

References

[1] Balendhran S, Walia S, Nili H, Sriram S and Bhaskaran M 2015 Elemental analogues of graphene: silicene, germanene, stanene, and phosphorene *Small* **11** 640–52
[2] Xu M, Liang T, Shi M and Chen H 2013 Graphene—like two-dimensional materials *Chem. Rev.* **113** 3766–98
[3] Das S, Robinson J A, Dubey M, Terrones H and Terrones M 2015 Beyond graphene: progress in novel two-dimensional materials and van der waals solids *Ann. Rev. Mater. Res.* **45** 1–27
[4] Novoselov K S A, Geim A K, Morozov S V B, Jiang D, Katsnelson M I C, Grigorieva I V A, Dubonos S V B and Firsov A A B 2005 Two-dimensional gas of massless dirac fermions in graphene *Nature* **438** 197–200
[5] Geim A K and Grigorieva I V 2013 Van der waals heterostructures *Nature* **499** 419–25
[6] Zhang Y J, Yoshida M, Suzuki R and Iwasa Y 2015 2d crystals of transition metal dichalcogenide and their iontronic functionalities *2D Mater.* **2** 044004
[7] Balandin A A, Ghosh S, Bao W, Calizo I, Teweldebrhan D, Miao F and Lau C N 2008 Superior thermal conductivity of single-layer graphene *Nano Lett.* **8** 902–7
[8] Zolyomi V, Wallbank J R and Fal'ko V I 2014 Silicane and germanane: tight-binding and first-principles studies *2D Mater.* **1** 011005
[9] Lorenz T, Joswig J-O and Seifert G 2014 Stretching and breaking of monolayer MoS_2—an atomistic simulation *2D Mater.* **1** 011007
[10] Liu F, Ming P and Li J 2007 *Ab initio* calculation of ideal strength and phonon instability of graphene under tension *Phys. Rev.* B **76** 064120
[11] Grantab R, Shenoy V B and Ruoff R S 2010 Anomalous strength characteristics of tilt grain boundaries in graphene *Science* **330** 946–8
[12] Chang T and Gao H 2003 Size-dependent elastic properties of a single-walled carbon nanotube via a molecular mechanics model *J. Mech. Phys. Solids* **51** 1059–74
[13] Scarpa F, Adhikari S and Srikantha Phani A 2009 Effective elastic mechanical properties of single layer graphene sheets *Nanotechnology* **20** 065709
[14] Shokrieh M M and Rafiee R 2010 Prediction of young's modulus of graphene sheets and carbon nanotubes using nanoscale continuum mechanics approach *Mater. Des.* **31** 790–5
[15] Boldrin L, Scarpa F, Chowdhury R and Adhikari S 2011 Effective mechanical properties of hexagonal boron nitride nanosheets *Nanotechnology* **22** 505702

[16] Le M-Q 2015 Prediction of young's modulus of hexagonal monolayer sheets based on molecular mechanics *Int. J. Mech. Mater. Des.* **11** 15–24
[17] Li C and Chou T-W 2006 Static and dynamic properties of single-walled boron nitride nanotubes *J. Nanosci. Nanotechnol.* **6** 54–60
[18] Huang C, Chen C, Zhang M, Lin L, Ye X, Lin S, Antonietti M and Wang X 2015 Carbon-doped bn nanosheets for metal-free photoredox catalysis *Nat. Commun.* **6** 7698
[19] Vogt P, Padova P D, Quaresima C, Avila J, Frantzeskakis E, Asensio M C, Resta A, Ealet B and Lay G L 2012 Silicene: compelling experimental evidence for graphenelike two-dimensional silicon *Phys. Rev. Lett.* **108** 155501
[20] van den Broek B, Houssa M, Iordanidou K, Pourtois G, Afanasev V V and Stesmans A 2016 Functional silicene and stanene nanoribbons compared to graphene: electronic structure and transport *2D Mater.* **3** 015001
[21] Ni Z, Liu Q, Tang K, Zheng J, Zhou J, Qin R, Gao Z, Yu D and Lu J 2012 Tunable bandgap in silicene and germanene *Nano Lett.* **12** 113–8
[22] Liu H, Neal A T, Zhu Z, Luo Z, Xu X, Tomnek D and Ye P D 2014 Phosphorene: an unexplored 2d semiconductor with a high hole mobility *ACS Nano* **8** 4033–41
[23] Zhu F, Chen W, Xu Y, Gao C, Guan D, Liu C, Qian D, Zhang S C and Jia J 2015 Epitaxial growth of two-dimensional stanene *Nat. Mater.* **14** 1020–5
[24] Mannix A J *et al* 2015 Synthesis of borophenes: anisotropic, two-dimensional boron polymorphs *Science* **350** 1513–6
[25] Brunier T M, Drew M G B and Mitchell P C H 1992 Molecular mechanics studies of molybdenum disulphide catalysts parameterisation of molybdenum and sulphur *Mol. Simul.* **9** 143–59
[26] Zhao W, Ghorannevis Z, Chu L, Toh M, Kloc C, Tan P-H and Eda G 2013 Evolution of electronic structure in atomically thin sheets of ws2 and wse2 *ACS Nano* **7** 791–7
[27] Coehoorn R, Haas C, Dijkstra J, Flipse C J F, de Groot R A and Wold A 1987 Electronic structure of $mose_2$, mos_2, and wse_2. I. Band-structure calculations and photoelectron spectroscopy *Phys. Rev.* B **35** 6195–202
[28] Ruppert C, Aslan O B and Heinz T F 2014 Optical properties and band gap of single- and few-layer mote2 crystals *Nano Lett.* **14** 6231–6
[29] Gelin B R 1994 *Molecular Modeling of Polymer Structures and Properties* (New York: Hanser Gardner Publications)
[30] Gibson L J and Ashby M F 1999 *Cellular Solids Structure and Properties* (Cambridge: Cambridge University Press)
[31] Mukhopadhyay T and Adhikari S 2016 Equivalent in-plane elastic properties of irregular honeycombs: An analytical approach *Int. J. Solids Struct.* **91** 169–84
[32] Mukhopadhyay T and Adhikari S 2016 Effective in-plane elastic properties of auxetic honeycombs with spatial irregularity *Mech. Mater.* **95** 204–22
[33] Mukhopadhyay T and Adhikari S 2016 Free vibration analysis of sandwich panels with randomly irregular honeycomb core *J. Eng. Mech.* **10** 06016008
[34] Mukhopadhyay T and Adhikari S 2017 Stochastic mechanics of metamaterials *Compos. Struct.* **162** 85–97
[35] Li C and Chou T W 2003 A structural mechanics approach for the analysis of carbon nanotubes *Int. J. Solids Struct.* **40** 2487–99
[36] Roark R J and Young W C 1976 *Formulas for Stress and Strain* (New York: McGraw-Hill)
[37] Cornell W D, Cieplak P, Bayly C I, Gould I R, Merz K M, Ferguson D M, Spellmeyer D C, Fox T, Caldwell J W and Kollman P A 1995 A second generation force field for the simulation of proteins, nucleic acids, and organic molecules *J. Am. Chem. Soc.* **117** 5179–97
[38] Lee C, Wei X, Kysar J W and Hone J 2008 Measurement of the elastic properties and intrinsic strength of monolayer graphene *Science* **321** 385–8
[39] Demczyk B G, Wang Y M, Cumings J, Hetman M, Han W, Zettl A and Ritchie R O 2002 Direct mechanical measurement of the tensile strength and elastic modulus of multiwalled carbon nanotubes *Mater. Sci. Eng.* A **334** 173–8
[40] Kudin K N, Scuseria G E and Yakobson B I 2001 c_2f, bn, and c nanoshell elasticity from *ab initio* computations *Phys. Rev.* B **64** 235406
[41] Lier G V, Alsenoy C V, Doren V V and Geerlings P 2000 *Ab initio* study of the elastic properties of single-walled carbon nanotubes and graphene *Chem. Phys. Lett.* **326** 181–5
[42] Sánchez-Portal D, Artacho E, Soler J M, Rubio A and Ordejón P 1999 *Ab initio* structural, elastic, and vibrational properties of carbon nanotubes *Phys. Rev.* B **59** 12678–88
[43] Jiang J-W, Wang J-S and Li B 2009 Young's modulus of graphene: a molecular dynamics study *Phys. Rev.* B **80** 113405
[44] Zhao H, Min K and Aluru N R 2009 Size and chirality dependent elastic properties of graphene nanoribbons under uniaxial tension *Nano Lett.* **9** 3012–5
[45] Modarresi M, Kakoee A, Mogulkoc Y and Roknabadi M R 2015 Effect of external strain on electronic structure of stanene *Comput. Mater. Sci.* **101** 164–7
[46] Bertolazzi S, Brivio J and Kis A 2011 Stretching and breaking of ultrathin MoS_2 *ACS Nano* **5** 9703–9
[47] Song L *et al* 2010 Large scale growth and characterization of atomic hexagonal boron nitride layers *Nano Lett.* **10** 3209–15
[48] Peng Q, Ji W and De S 2012 Mechanical properties of the hexagonal boron nitride monolayer: *ab initio* study *Comput. Mater. Sci.* **56** 11–7
[49] Zhao S and Xue J 2013 Mechanical properties of hybrid graphene and hexagonal boron nitride sheets as revealed by molecular dynamic simulations *J. Phys. D: Appl. Phys.* **46** 135303
[50] Le M-Q 2014 Young's modulus prediction of hexagonal nanosheets and nanotubes based on dimensional analysis and atomistic simulations *Meccanica* **49** 1709–19
[51] Jiang L and Guo W 2011 A molecular mechanics study on size-dependent elastic properties of single-walled boron nitride nanotubes *J. Mech. Phys. Solids* **59** 1204–13
[52] Oh E S 2011 Elastic properties of various boron-nitride structures *Met. Mater. Int.* **17** 21–7
[53] Castellanos-Gomez A, Poot M, Steele G A, van der Zant H S J, Agraít N and Rubio-Bollinger G 2012 Elastic properties of freely suspended mos2 nanosheets *Adv. Mater.* **24** 772–5
[54] Lorenz T, Teich D, Joswig J-O and Seifert G 2012 Theoretical study of the mechanical behavior of individual TiS2 and MoS2 nanotubes *J. Phys. Chem.* C **116** 11714–21
[55] Scalise E, Houssa M, Pourtois G, Afanas'ev V and Stesmans A 2012 Strain-induced semiconductor to metal transition in the two-dimensional honeycomb structure of mos2 *Nano Res.* **5** 43–8
[56] Jiang J-W, Qi Z, Park H S and Rabczuk T 2013 Elastic bending modulus of single-layer molybdenum disulfide (MoS_2): finite thickness effect *Nanotechnology* **24** 435705
[57] Blakslee O L, Proctor D G, Seldin E J, Spence G B and Weng T 1970 Elastic constants of compression-annealed pyrolytic graphite *J. Appl. Phys.* **41** 3373–82
[58] Tu Z-C and Ou-Yang Z-C 2002 Single-walled and multiwalled carbon nanotubes viewed as elastic tubes with the effective young's moduli dependent on layer number *Phys. Rev.* B **65** 233407
[59] Brenner D W 1990 Empirical potential for hydrocarbons for use in simulating the chemical vapor deposition of diamond films *Phys. Rev.* B **42** 9458–71
[60] Alzebdeh K 2012 Evaluation of the in-plane effective elastic moduli of single-layered graphene sheet *Int. J. Mech. Mater. Des.* **8** 269–78
[61] Alzebdeh K I 2014 An atomistic-based continuum approach for calculation of elastic properties of single-layered graphene sheet *Solid State Commun.* **177** 25–8
[62] Sakhaee-Pour A 2009 Elastic properties of single layered graphene sheet *Solid State Commun.* **149** 91–5
[63] Akdim B, Pachter R, Duan X and Wade Adams W 2003 Comparative theoretical study of single-wall carbon and boron-nitride nanotubes *Phys. Rev.* B **67** 245404

[64] Verma V, Jindal V K and Dharamvir K 2007 Elastic moduli of a boron nitride nanotube *Nanotechnology* **18** 435711
[65] Oh E-S 2010 Elastic properties of boron-nitride nanotubes through the continuum lattice approach *Mater. Lett.* **64** 859–62
[66] Woo S, Park H C and Son Y-W 2016 Poisson's ratio in layered two-dimensional crystals *Phys. Rev.* B **93** 075420
[67] Mayo S L, Olafson B D and Goddard W A 1990 Dreiding: a generic force field for molecular simulations *J. Phys. Chem.* **94** 8897–909
[68] Bosak A, Serrano J, Krisch M, Watanabe K, Taniguchi T and Kanda H 2006 Elasticity of hexagonal boron nitride: inelastic x-ray scattering measurements *Phys. Rev.* B **73** 041402
[69] Wang D, Chen L, Wang X, Cui G and Zhang P 2015 The effect of substrate and external strain on electronic structures of stanene film *Phys. Chem. Chem. Phys.* **17** 26979–87
[70] Tang P, Chen P, Cao W, Huang H, Cahangirov S, Xian L, Xu Y, Zhang S-C, Duan W and Rubio A 2014 Stable two-dimensional dumbbell stanene: a quantum spin hall insulator *Phys. Rev.* B **90** 121408
[71] van den Broek B, Houssa M, Scalise E, Pourtois G, Afanasev V V and Stesmans A 2014 Two-dimensional hexagonal tin: *ab initio* geometry, stability, electronic structure and functionalization *2D Mater.* **1** 021004
[72] Radisavljevic B, Radenovic A, Jacopo Brivio, Giacometti I V and Kis A 2011 Single-layer mos2 transistors *Nat. Nanotechnol.* **6** 147–50
[73] Bronsema K D, Boer J L D and Jellinek F 1986 On the structure of molybdenum diselenide and disulfide *Z. Anorg. Allg. Chem.* **540** 15–7
[74] Schönfeld B, Huang J J and Moss S C 1983 Anisotropic mean-square displacements (msd) in single-crystals of 2h-and 3r-mos2 *Acta Crystallogr.* B **39** 404–7
[75] Wieting T J and Verble J L 1971 Infrared and raman studies of long-wavelength optical phonons in hexagonal mos2 *Phys. Rev.* B **3** 4286
[76] Ma Z X and Dai S S 1989 *Ab initio* studies on the electronic structure of the complexes containing mo's bond using relativistic effective core potentials *Acta Chim. Sin. Engl. Ed.* **7** 201–8
[77] Castellanos-Gomez A, van Leeuwen R, Buscema M, van der Zant H S J, Steele G A and Venstra W J 2013 Single-layer mos2 mechanical resonators *Adv. Mater.* **25** 6719–23
[78] Li T 2012 Ideal strength and phonon instability in single-layer MoS_2 *Phys. Rev.* B **85** 235407